EDDY CURRENTS, MAGNETIC FLUX AND FORCE IN SOLID MAGNETIC THRUST BEARINGS

Paul E. Allaire
Roger L. Fittro
Eric H. Maslen
Mechanical, Aerospace and Nuclear Engineering Dept
University of Virginia, Charlottesville, Virginia, USA

William C. Wakefield
Proctor & Gamble, Hunt Valley, Maryland, USA

NOMENCLATURE

A_g pole cross sectional area (one pole)
b_1 hysteresis offset
b_2 - equivalent iron gap offset
B - magnetic flux density
D_1 - bearing inner diameter
D_2 - coil inner diameter
D_3 - coil outer diameter
D_4 - bearing outer diameter
F - force
F_0 - nominal force
g - air gap (one)
g_0 - nominal air gap
H_c - coercive force (field intensity)
I - current
I_c - effective current
I_0 - nominal current
L - total axial length
L_c - thrust collar length
L_i - length of magnetic path in iron
N - number of turns
γ - force proportionality constant
μ_0 - permeability of free space
μ_r - relative permeability

ABSTRACT

This paper discusses the force/current relation for a solid magnetic thrust bearing. The particular bearing was designed for a laboratory pump as a bearing/load cell to support the shaft as well as measure the thrust forces on the impeller. The current/force relation is also important for magnetic bearings installed in pumps, compressors, and other rotating machines where the measured current level can be used to determine operating force levels.

A non-rotating test rig was constructed to directly measure the force as the current was cycled through major and minor loops for various air gaps. Quasi-static major current loops at a rate of 0.1 A/sec exhibited differences in measured forces of up to 12.6% between increasing and decreasing current trajectories. A dimensionless curve fit was developed for the data, with an error of approximately 4 percent. A bimodal error distribution was found which corresponds to magnetic hysteresis in the magnetic bearing. The error is dependent upon the current/force path followed during the current cycle and represents an uncertainty in the force measurement.

Current cycles at frequencies of 0.1 to 40 Hz were also tested and produced differences of up to 34.9%. Plots of magnitude and phase were obtained from the sinusoidal data which showed that the magnitude of the current/force ratio is relatively constant at low frequencies but decreases by 28% at 40 Hz. The phase angle exhibits a relatively large phase lag of approximately 16 degrees at 40 Hz.

INTRODUCTION

The current/force relation is an important topic for magnetic bearings. Normally a magnetic thrust bearing is employed to provide an axial load capacity in a rotating machine [Allaire, 1989a]. Fig. 1 shows the geometry of a magnetic thrust bearing. Proper design of the bearing requires detailed knowledge of the force which results when a current is applied. Simple magnetic circuit analysis is often employed for preliminary thrust bearing design [Allaire, et al., 1994a]. Many effects such as nonlinearities, eddy currents, hysteresis, fringing, leakage, and frequency effects are not included in these simple models. Knowledge of the phase lag found in the thrust bearing affects the feedback control loop design. One purpose of this paper is to investigate some of these effects by measuring the properties of a particular bearing.

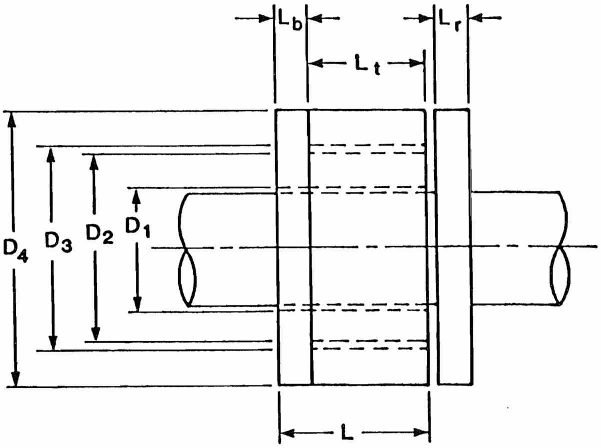

FIGURE 1: Side View of Thrust Bearing

When magnetic bearings are employed in a pump [Allaire, et al., 1989b], compressor, turbine or other rotating machine, knowledge of the forces imposed on the bearings can be a significant indicator of machine problems. The forces are directly related to the currents in the bearings. A thrust bearing was designed for the purpose of measuring thrust forces in an impeller. This paper discusses the current/force relation for the magnetic thrust bearing. Force measurements were made in the test rig as the bearing coil currents were cycled at various time rates of change.

Test rigs have been developed for measuring thrust and radial forces by several investigators. An example paper is given by Jery, et al. [1985] reporting on a strain gage based test rig. Rigs of this type require very careful construction to minimize structural interactions which contribute to uncertainties in the measurements. Testing has also been limited to impellers with relatively large clearances compared to industrial practice.

Magnetic bearings have begun to be used for purposes other than supporting a shaft. The use of a magnetic bearing as an excitation force has been described by Ulbrich [1988]. Wagner and Pietruszka [1988] developed a magnetic bearing to be used for the measurement of fluid forces in turbocompressor applications. Hawkins, et al. [1991] have also employed magnetic bearings as a known force input device for the identification of rotor dynamic coefficients in a test stand. Feng, et al. [1992] and Verhoeven, et al. [1993] employed magnetic bearings in two test rigs for the identification of long seals and impeller/casing interactions. Hawkins and Imlach [1993] described an experimental method for the measurement of the frequency dependent force displacement transfer function of a magnetic bearing/controller system.

As noted above, quite a few works on using magnetic bearings to measure or identify external forces in rotating machinery have been reported in the literature over the past decade. All of these projects depend upon the current/force relation in the magnetic bearings. However, there have been few studies reported on accurately determining the characteristics of this relation for specific magnetic bearing configurations. Hysteresis and eddy current effects can be important in magnetic bearing characterization. The B-H curve of any magnetic material exhibits hysteresis which affects the current/force relation. A hysteresis curve for a typical magnetic material is shown in Fig. 2. The increasing H values follow a different curve than the decreasing H values. The area between the curves represents the energy loss during the cycle.

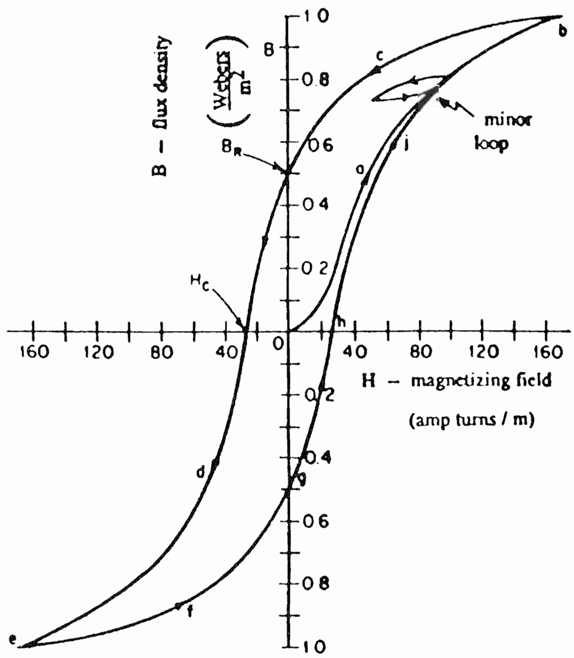

FIGURE 2: B-H Curve for Typical Magnetic Material

Eddy current effects degrade magnetic bearing performance [Zmood, et al., 1987]. Williams and Trumper [1993] have investigated material/air gap hysteresis effects in a laminated stack similar to a radial bearing. Keith [1993] conducted an extensive study of eddy current and hysteresis effects on current/force relations in a two pole magnetic configuration similar to a magnetic bearing. He found that eddy current effects in solid pole pieces, with a 0.51 mm (10 mils) gap, dominated the current/force relation as the frequency increased above approximately 2 Hz. Keith [1993] noted that this produces a significant phase lag in the actuator.

If a magnetic thrust bearing is perfectly axisymmetric and the coil currents are held constant, there will be no eddy current effects present. However, thrust bearings in industrial use are subject to time varying forces.

The coil currents are changed to adjust the bearing force in response to the applied load. These time varying currents generate hysteresis and eddy current effects in thrust bearings. In turn, these induced eddy currents produce induced magnetic fields opposing the applied magnetic field. These effects were studied in the magnetic thrust bearing described here. Both of these phenomena affect the current/force relation in operating industrial bearings.

THRUST BEARING CONFIGURATION

The geometry of a magnetic thrust bearing is shown in Fig. 1. The stator is composed of an inner toroid, a base plate, outer toroid, and a coil of wire. The rotor is simply a flat disk fixed to the shaft (also called a thrust disk or thrust runner). The stator may be solid or divided into sectors to reduce eddy currents. This work considers only solid thrust bearing components.

A magnetic thrust bearing was designed for a thrust load of 187 N (42 lbf). The inner and outer diameters are given in Table 1 as well as other bearing dimensions. The operating current (design bias current) was 1.75 A and the nominal operating air gap of the bearing was 0.762 mm (0.030 in). All magnetic components were constructed of conventional solid soft iron material rather than laminated. The coils consisted of 300 turns secured in the bearing by a thin nonmagnetic stainless steel retainer.

TEST APPARATUS

An Instron Universal Testing machine was utilized for the measurements. A load cell was attached to the moveable crosshead and the thrust bearing fixed to the base of the machine. Figure 3 shows a drawing of the test set up. Calibration of the testing apparatus was accomplished by hanging known weights from the collar holder and measuring the force. Great care, using shims around the circumference of the bearing, was taken to ensure that the thrust collar and bearing were parallel. The current in the bearing coil was cycled at different frequencies and for different air gaps.

A computer was employed as a data acquisition device. The computer was programmed to cycle the current through the thrust bearing coil, record the test data in a file, and present it graphically. It was possible to examine individual data points for each experiment, thus making the comparison of forces at various points simple and accurate.

QUASI-STATIC CURRENT CYCLE TEST RESULTS

Force vs. current measurements were made for a wide range of air gaps and currents. Current cycles were run at a quasi-static rate of 0.1 A/sec to evaluate primarily hysteresis effects. Lower current rates were tried with essentially the same results. Two major current loop tests were run. Figure 4 shows force/current values for an air gap of 0.762 mm (30 mils) and a major current loop from -2.55 A to 2.55 A. For the same air gap, two loops of 0.95 A to 2.55 A and 1.35 A to 2.15 A were tested. The results are given in Figures 5 and 6. Many other tests were run but are not presented here.

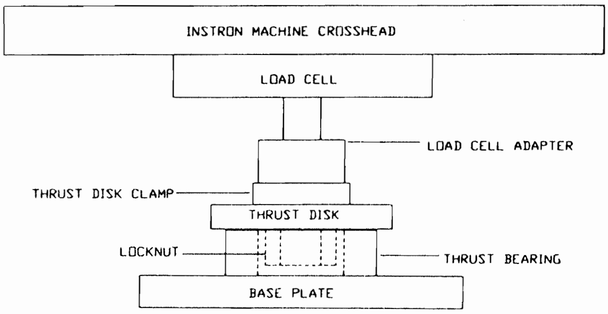

FIGURE 3: Drawing of Thrust Bearing Test Setup

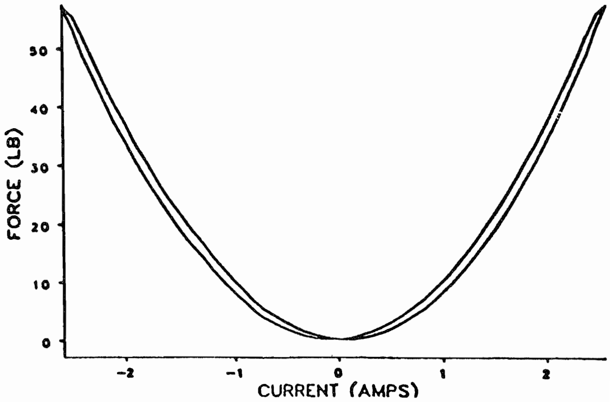

FIGURE 4: Measured Force vs. Current with Air Gap 0.762 mm (0.030 in), Current -2.55 A to 2.55 A

The shape of each force/current plot was the same for increasing and decreasing currents. For comparison purposes, the force was evaluated at the design bias current value of 1.75 A as the perturbation current was increasing and decreasing. The difference between the two curves was as high as 12.6% for major current loops but reduced to 4.7% for minor loops more likely to be encountered in actual use. The repeatability of the curves was very high. The two sided nature of the curves is due to hysteresis because the time rate of change of the current was so low.

TABLE 1. Design Parameters for Magnetic Thrust Bearing

Design Parameter	Value
Outer Diameter, D_4	91.4 mm/3.60 in
Inner Diameter, D_1	44.4 mm/1.75 in
Total Axial Length, L	26.4 mm/1.04 in
Thrust Collar Length, L_c	14.2 mm/0.56 in
Design Air Gap, g	0.762 mm/0.030 in
Design Bias Current, I_b	1.75 A
Number of Turns/Wire Gage	300 turns/#22 wire
Design Steady State Load Capacity, F_s	187 N/42 lbf
Design Perturbation Current, I_p	+/- 0.85 A (0.95 A to 2.55 A)

CURRENT/FORCE EQUATION

Single sided magnetic bearings are nonlinear with the force related to the square of the coil currents [Allaire, et al., 1994b]. When the bearing is double acting, the net effect is to linearize the actuator so that the force-current relation is linear. The flux density B in the magnetic circuit is given by

$$B = \frac{N(I + I_c)}{A_g\,(2\mathcal{R}_g + \mathcal{R}_i)} \tag{1}$$

where the air gap and iron reluctances are given by

$$\mathcal{R}_g = \frac{g}{\mu_0 A_g} \qquad \mathcal{R}_i = \frac{L_i}{\mu_0 \mu_r A_g} \tag{2}$$

As the H value decreases, the material will have a coercive force H_c remaining when zero magnetic flux density is reached. This may be represented as an effective current I_c where

$$I_c = \frac{H_c}{N} L = \frac{H_c}{N}(2g + L_i) \tag{3}$$

This corresponds to the current required to return the magnetic flux density B to zero. Of course, in the magnetic bearing this material effect is combined with the air gap, which has no hysteresis, to greatly reduce the difference between the increasing and decreasing parts of the B-H curve for the overall bearing. As the material has the magnetic field intensity H decreased gradually, the B-H curve will return to the origin of the B-H plot. However, if the bearing is operated so that it has a coercive force, the flux equation (1) must include the corresponding current.

The force F which attracts the rotor to the stator is given by

$$F(I,g) = \frac{\mu_0 N^2 (I + I_c)^2 A_g}{4\left(g + \frac{L_i}{2\mu_r}\right)^2} \tag{4}$$

The force is proportional to the square of $N(I + I_c)$ and inversely proportional to the square of gap g plus a constant. This is in the general form employed here.

There is an operating point for the thrust bearing with current I_0 and gap g_0. Let the nominal force be that due to the air gap reluctance only with the result:

$$F_0 = \frac{\mu_0 N^2 I_0^2 A_g}{4 g_0^2} \tag{5}$$

For the bearing tested in this work, $I_0 = 1.75$ A, $g_0 = 0.762$ mm (30 mils) and $F_0 = 203.8$ N (45.8 lb). Define the dimensionless force as:

$$\bar{F}(\bar{I},\bar{g}) = \frac{\left(\bar{I} + \frac{I_c}{I_0}\right)^2}{\left(\bar{g} + \frac{L_i}{2\mu_r g_0}\right)^2} \quad \text{where } \bar{I} = \frac{I}{I_0},\ \bar{g} = \frac{g}{g_0} \tag{6}$$

This suggests the generic form of the current/force relation employed in this paper to fit the measured data for the tested single sided magnetic thrust bearing:

$$\bar{F}(\bar{I},\bar{g}) = \gamma\left(\frac{\bar{I} + b_1}{\bar{g} + b_2}\right)^2 \tag{7}$$

The primary variables are the current and air gap length. Here γ is a dimensionless constant of proportionality, b_1 represents an offset in the B-H curve for the magnetic material due to hysteresis effects and b_2 the ratio of equivalent magnetic length to the nominal air gap.

A least squares curve fit of the data from the thrust bearing measurements produced the following values for the current/force equation:

$$\gamma = 0.996 \qquad b_1 = 0.0718 \qquad b_2 = 0.3247 \tag{8}$$

Figure 5 shows a comparison of the curve fit with one of the measured current loops. The zero point indicates the equivalent coercive current I_c. Unfortunately, the relative permeability of the magnetic material has not yet been measured so a comparison with the theoretical model of Eq. (6) is not possible at the time of writing this paper.

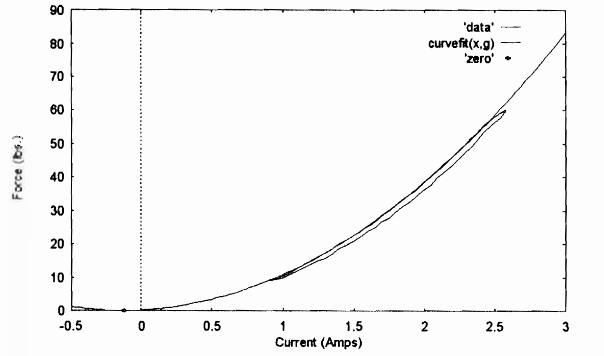

FIGURE 5: Measured Force vs. Current with Air Gap 0.762 mm (0.030 in), Current -0.95 A to 2.55 A and Least Squares Curve Fit (to All Data)

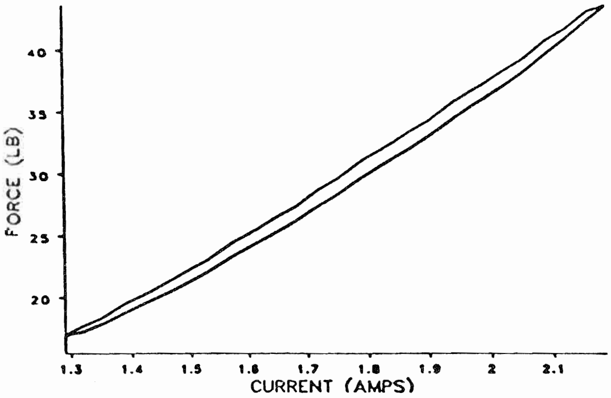

FIGURE 6: Measured Force vs. Current With Air Gap 0.762 mm (0.030 in), Current 1.35 A to 2.15A

Many data runs were employed to develop the curve fit. In each case, only measurements with the design current range, 0.95 A to 2.55 A, were used, with the current changing at 0.1 A/sec. Equal numbers of increasing and decreasing current data were averaged to produce the numerical values in Eq. (8). Figure 7 shows the deviation between the actual data and that predicted by Eq. (7). The distribution of error is noticeably bimodal with a mean of 0.3 percent and a standard deviation of 3.8 percent. The bimodal distribution suggests the superposition of two normal distributions with differing mean values. The experimental data was taken for force/current trajectories essentially on the same hysteresis loop from 0.95 A to 2.55 A. The separation between the two halves of the hysteresis loops, one with increasing current and the other with decreasing current, is believed to have induced the bimodal distribution. Further, the resulting non-zero mean can be explained by the fact that a least squares curve fit minimizes the absolute error while the error, $[F(I, g) - F_{act}]/F_{act}$, plotted in Fig. 7 is normalized with respect to the actual force. Therefore, a zero mean cannot be expected.

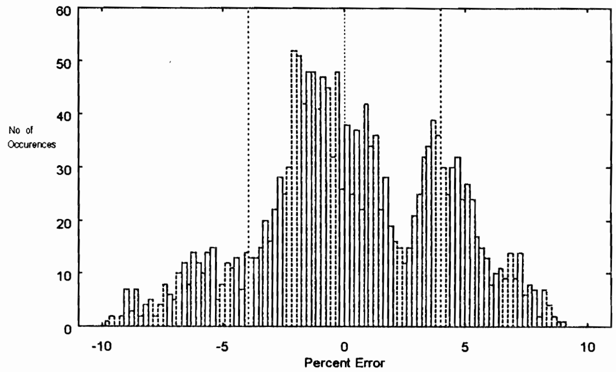

FIGURE 7: Error Distribution in Current/Force Curvefit

UNCERTAINTY ANALYSIS

An uncertainty analysis was conducted to determine the extent to which uncertainty in the calibration data produces uncertainty in the calibration parameters (γ, b_1, b_2) and the extent to which this model uncertainty, coupled with the measurement uncertainty during the execution of the actual experiment, will lead to uncertainty in the measured forces.

This uncertainty analysis was performed in a two step procedure. First, the uncertainty in the model parameters due to the data uncertainty was calculated. Then the total expected force uncertainty was calculated based on these values. This analysis resulted in an expected mean error of zero and a standard deviation of 3.96 percent. These results are graphically displayed in Fig. 7 by the dashed vertical lines. This result is consistent with the observed distributions about the two modal means, implying that the only major (non-random) source of error in the measurements is due to hysteresis.

FREQUENCY EFFECTS

Eddy currents develop due to time varying currents in the bearing coil. The induced flux in the stator opposes the applied flux to reduce the generated magnetic bearing force. The resulting frequency response effects can cause a magnetic bearing performance to deviate significantly from expected values. The current was cycled through the design current loop of 0.95 A to 2.55 A at various frequencies. Figure 8 shows the force/current plots for 0.1, 1.0 and 10.0 Hz with an air gap of 0.762 mm (30 mils). The difference in the loop segments becomes larger as the frequency increases. This is due to higher eddy current effects as the time rate of change of the electric field increases. The largest difference measured was 34.9%. Similar plots were generated for other frequencies.

The ratio of force to current was evaluated for a range of frequencies. The current value vs. frequency was generated by comparison of the measured current signal to a sinusoidal reference. A similar method was used for the force value. A ratio of these values was then taken. The magnitude is plotted in Fig. 9 and the phase angle is plotted in Fig. 10. The magnitude is relatively constant over the frequency range up to 2 Hz but drops off approximately 28% at 40 Hz. The phase angle approximately follows a second order function with frequency. It drops off to approximately 16 degrees at 40 Hz. A least squares second order curve fit to the phase angle gives the results

$$\phi = -1.039\ \omega^{1/2} - 2.0135 \qquad (15)$$

as shown in Fig. 10. A linear model was also curve fit to the data as illustrated in Fig. 10 but the fit is not very good.

The pump in which these bearings will be employed runs at approximately 10 Hz with a blade pass frequency of approximately 40 Hz. Overall, the large drop off of phase angle at the running frequency and blade pass frequency makes this particular bearing a relatively poor choice for the purpose of measuring pump forces.

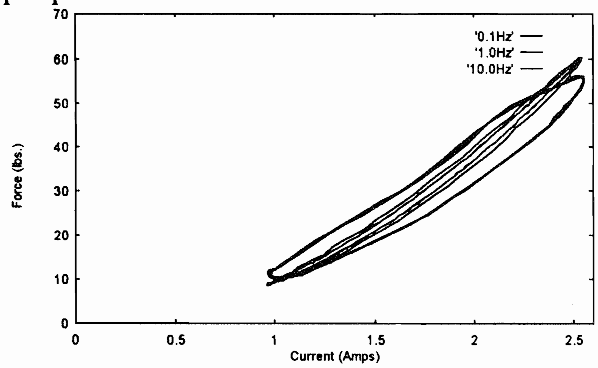

FIGURE 8: Measured Force vs. Sinusoidal Current At 0.1, 1.0, 10 Hz With Air Gap 0.762 mm (0.030 in) Current 0.95 A to 2.55 A

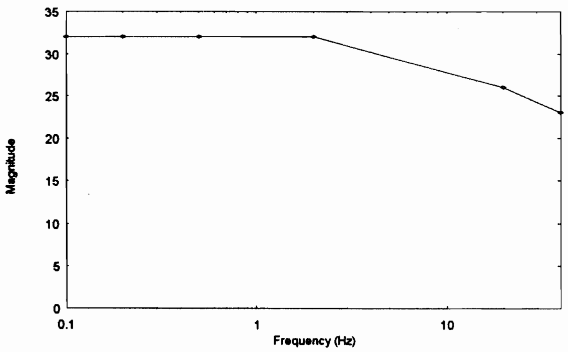

FIGURE 9: Magnitude of Force/Current Ratio

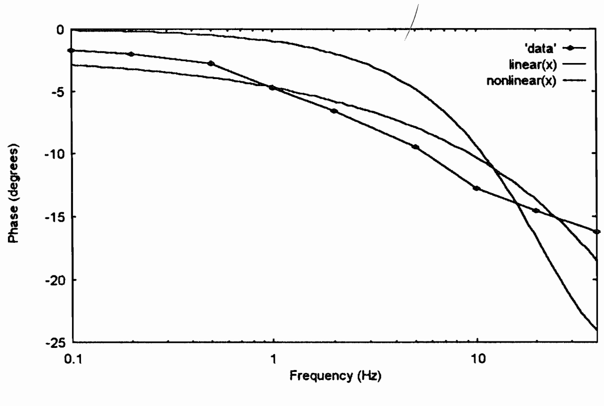

FIGURE 10: Phase Angle of Force/Current Ratio with Curve Fits

CONCLUSIONS

Numerous papers, noted in the introduction, either propose or have reported the use of magnetic bearings to determine external forces in a rotating machine or component. However, not much has been reported in the literature on verifying the theoretical equations apparently employed to extract the data. The deviations from the simple force/current relations normally quoted for magnetic thrust bearing load capacity must be taken into account when using magnetic bearings as load cells. Testing must be carried out and magnetic bearings redesigned to reduce uncertainties or their usefulness is questionable.

A solid magnetic thrust bearing was constructed and tested. The quasi-static force vs. current relations were measured for a variety of air gaps and currents. The thrust bearing exhibits a hysteresis effect which creates a significant difference between force measurements when the current is increasing or decreasing. For major current loops, from -2.55 A to 2.55 A, changing at a rate of 0.1 A/sec, the maximum force difference varied from 6% to 11%. For design current loops, 0.95 A to 2.55 A, at the same time rate of change, the difference ranged from 4% to 8%. At this low time rate of change of current, this difference is due to material hysteresis effects. A dimensionless curve fit expression was obtained for this quasi-static data with a mean error of 0.3 percent and a standard deviation of 3.8 percent.

It is important to discuss the significance of the bimodal nature of the error in regard to the measurement of pump force. If the bearing is operated in small trajectories about a fixed (non-zero) operation point on the F/I (force/current) curve, the scatter in the error could be expected to be on the order of 4 percent, but the error will not have a zero mean. Further, the actual mean error will depend upon the specific F/I trajectory used to reach the operating point. As seen in the error distribution, the mean error could well be on

A sinusoidal perturbation current was also imposed on the thrust bearing. Force/current magnitude and phase angle values vs. frequency were obtained for the bearing. The magnitude was relatively constant up to 2 Hz but then decreased with frequency. The phase lag was determined to increase with frequency with a value of 16 degrees at 40 Hz. As the frequency increases, eddy currents are induced in the solid thrust bearing components. These eddy currents must be reduced in order to be able to accurately measure pump forces over a wide frequency range with magnetic bearings. One option to be explored is division of the solid stator into segments to reduce the eddy currents.

REFERENCES

Allaire, P. E., 1989a, "Design and Test of a Magnetic Thrust Bearing," Journal of the Franklin Institute, Vol. 326, No. 6, December.

Allaire, P., Imlach, J., McDonald, J., Humphris, R., Lewis, D., Blair, B., Claydon, J. and Flack, R., 1989b "Design, Construction and Test of a Magnetic Bearing in an Industrial Canned Motor Pump," Proc. of Texas A&M Pump Symposium, Houston, TX, May.

Allaire, P. E., Maslen, E. H., Humphris, R. R., Knospe, C. R., and Lewis, D. W., 1994a, "Magnetic Bearings," Handbook of Lubrication and Tribology, Vol. III, CRC Press, pp. 577-600.

Allaire, P. E., Maslen, E. H., Lewis, D. W., and Flack, R. D., 1994b, "Magnetic Thrust Bearing Operation and Industrial Pump Application,", Presented at ASME Turbo Expo '94 - Land, Sea & Air Conference, The Hague, Netherlands, June 13-16.

Feng, T., Neumer, T., Nordman, R., Verhoeven, J., and De Vis, D., 1992, "Identification of Fluid/Structure Interactions in Centrifugal Pumps," Fifth Intl. Conference on Vibrations in Rotating Machinery, Bath, England, 7-10 September.

Hawkins, L. A., Murphy, B. T., Lang, K. W., 1991, "The Rocketdyne Multifunction Tester: Operation of a Radial Magnetic Bearing as an Excitation Source," ROMAG '91 Proc., Magnetic Bearings and Dry Gas Seals International Conference, University of Virginia, March 13-15, pp. 1-13.

Hawkins, L. A., and Imlach, J., 1993, "Development of Experimental Method for Measurement of Magnetic Bearing Transfer Function Characteristics," Proc. of MAG '93, Magnetic Bearings, Magnetic Drives, and Dry Gas Seals Conference & Exhibition, July, Technomics Publishing Co., pp. 188-197.

Jery, B., Brennan, C. E., Caughey, T. E. and Acosta, A. J., 1985, "Forces in Centrifugal Pump Impellers," Proc. of Second Intl. Pump Symposium, Texas A&M University, pp. 21-29.

Keith, F. J., 1993, Implicit Flux Feedback Control for Magnetic Bearings, Ph.D. Dissertation, University of Virginia, May.

Ulbrich, H., 1988, "New Test Techniques Using Magnetic Bearings," Proc. First Intl. Symp. on Magnetic Bearings, June, Springer-Verlag, pp. 281-289.

Verhoeven, J. J., De Vis, D., and Nordman, R., 1993, "Development and Operating Experience of a 5000 KW Test Boilerfeed Pump on Active Magnetic Bearings," Proc. of Mechanical Engineers, C439/004.

Wagner, N. G., and Pietruszka, W. D., 1988, "Identification of Rotor Dynamic Parameters on a Test Stand with Active Magnetic Bearings," Proc. First Intl. Symp. on Magnetic Bearings, June, Springer-Verlag, pp. 289-302.

Williams, M. E., and Trumper, D. L., 1993, "Materials for Efficient High-Flux Magnetic Bearing Actuators," NASA Conference on Magnetic Suspension, Seattle, WA, August.

Zmood, R. B., Anand, D. K., Kirk, J. A., 1987, "The Influence of Eddy Currents on Magnetic Actuator Performance," Proceedings of IEEE, Vol. 75, No. 2, February.